Application of Analytical Models to Estimate Soiling Losses in Photovoltaic Systems in a Semiarid Region

José Janiere S. Souza[1] and Paulo C. M. Carvalho[2]

[1] Federal Institute of Ceará, Campus Cedro, Cedro (Brazil)

[2] Electrical Engineering Department, Federal University of Ceará, Fortaleza (Brazil)

Abstract

This study evaluates the applicability of analytical models to estimate soiling losses in a photovoltaic (PV) plant in a semiarid region. Regularly cleaned and uncleaned modules are compared using Fixed Fill Factor Model (FFFM), Variable Fill Factor Model (VFFM) and Approximate Maximum Power Point Model (AMPPM). All models show low average difference between estimated and measured values, with VFFM standing out for its higher accuracy. However, seasonality impacts accuracy, highlighting the need for calibration based on local environmental conditions.

Keywords: Analytical Models, Photovoltaic Plant, Soiling Losses

1. Introduction

The energy transition and the growing demand for electricity have driven the use of photovoltaic (PV) systems as a solution to reduce greenhouse gas emissions, as they provide clean, reliable, and scalable electricity production. However, PV conversion efficiency is affected by environmental, climatic, and anthropological factors, such as shading, temperature, and soiling (Ahmadullah *et al*., 2026). Soiling is a complex phenomenon characterized by the accumulation of contaminants (dust, particulate matter, animal excrement and snow, for example) on modules surface, causing a reduction of the glass transmittance and, consequently, negatively affecting their conversion performance (Ferrada *et al*., 2019; Souza; Carvalho; Pereira, 2023; Souza and Carvalho, 2025). Soiling is affected by different variables, such as modules installation angle, exposure period, local climatic conditions and physical-chemical-biological characteristics of the contaminants (Souza, Carvalho e Barroso, 2022). Depending on environmental conditions, soiling can cause energy losses ranging from 5% to more than 50%, making a PV plant unviable (Jones *et al*., 2016).

Models are found in the literature that use correlations between environmental variables (wind, humidity, temperature) and soiling information; some of them include modules tilt angle as a variable to model the soiling effect. Another widely used approach is the adoption of methods based on artificial intelligence, computational fluid dynamics, or image analysis techniques (Conceição *et al*., 2022; Cruz-Rojas *et al*., 2023; Brunel, *et al*., 2025). However, the number of factors influencing the soiling process tends to restrict such models to a specific location. For greater effectiveness in modeling soiling effects, studies should be based on data from at least one year of practical observations, incorporating the seasonal characteristics of the site. However, using data from a longer observation period allows for a more assertive analysis, detecting seasonal similarities in soiling rates across different years and, additionally, verifying their dependence on atmospheric parameters (Conceição *et al*., 2022). Therefore, continuous and regular monitoring of PV plants is necessary (Assis *et al*., 2025; Souza; Santos; Carvalho, 2025).

Several automated approaches have been proposed to reduce costs and human intervention, such as the use of soiling stations, optical sensors, image analysis sensors, and soiling extraction algorithms. However, implementing some of these solutions requires significant financial investment in the installation and/or acquisition stages. On the other hand, soiling effects extraction, in its simplest form, can be estimated using performance data or environmental parameters, even in locations where no PV module cleaning strategy is implemented (Bessa *et al*., 2021). In this context, the use of analytical models to estimate electrical parameters of clean PV systems and sequentially comparing them with values measured in unclean modules to verify soiling effects is an alternative for this type of study (Fernández-Solas *et al*., 2022). However, it is essential to evaluate the suitability and accuracy of these methods in relation to the actual values at the analyzed site.

In our paper we use models from Fernández-Solas *et al*. (2022), which uses analytical models to estimate the effects

10.18086/swc.2025.03.07 Available at http://proceedings.ises.org

of soiling on the environmental conditions of the University of Jaén (Spain), classified by the authors as low/moderate soiling levels. The study considers three different PV technologies: m-Si, CdTe, and CIS.

Given the above, the objective of our study is to verify the adequacy of analytical models to estimate electrical parameters of a PV plant in the Brazilian semiarid and their subsequent applicability for soiling studies. To validate the applicability of the analytical models, SRatio data are used, established by the ratio between the electrical power of a dirty module and the electrical power of a clean module under the same environmental and operational conditions. Unlike the methodology used by Fernández-Solas *et al*. (2022), this study does not use a dedicated experimental bench for this purpose, but rather data from a PV plant.

2. Materials and methods

2.1. Site of experimentation and system description

The outdoor experiments are carried out at the Alternative Energies Laboratory of the Federal University of Ceará (LEA-UFC) in Fortaleza, Brazil. An environmental characterization of Fortaleza for the period 2012–2022, based on meteorological data from the National Institute of Meteorology (INMET), obtained from a station approximately 10 km from the study site, and rainfall data, provided by the Ceará Foundation for Meteorology and Water Resources (FUNCEME), from a station about 2 km from LEA–UFC, indicates that the highest irradiation levels occur during the second half of the year, coinciding with the period of lowest rainfall (see Fig. 1). The annual average ambient temperature (TA) is 27.33°C, while the annual average relative humidity (UR) is 71.49% [86]. Tab. 1 presents the daily average values of global horizontal irradiance (GHI), TA and UR in Fortaleza in the period 2012–2022.

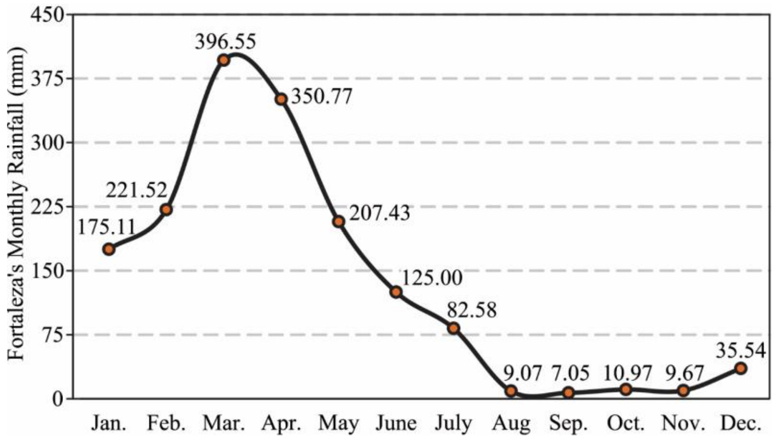

Fig. 1: Fortaleza's average monthly rainfall (2012-2022).

Tab. 2: Average daily values of GHI, TA and UR in Fortaleza (2012-2022).

-	Jan.	Fev.	Mar.	Apr.	May	June	July	Aug.	Sep.	Oct.	Nov.	Dec.
GHI (kWh/m^2)	4.93	4.89	4.47	4.44	4.52	4.51	4.68	5.43	5.78	5.86	5.67	5.29
TA (ºC)	27.68	27.55	27.17	27.08	27.06	26.83	26.57	26.95	27.30	27.72	27.99	28.10
UR (%)	72.39	74.57	78.03	78.61	76.32	73.38	71.04	66.86	65.98	65.78	66.64	68.25

The PV plant under investigation (LEA2) is composed by 12 p-Si modules distributed in two parallel strings, designated as ST1 and ST2. LEA2 uses an inverter with an integrated datalogger for electrical measurements. An IoT system acquires GHI, wind speed (WS), UR, TA and modules temperature (TM) data (Assis *et al*., 2025).

2.2. Manual cleaning (MC)

At the beginning of the study (July 5th, 2023) both strings are cleaned; LEA2 strings before, during and after performing manual cleaning (MC) procedures are shown in Fig. 2.

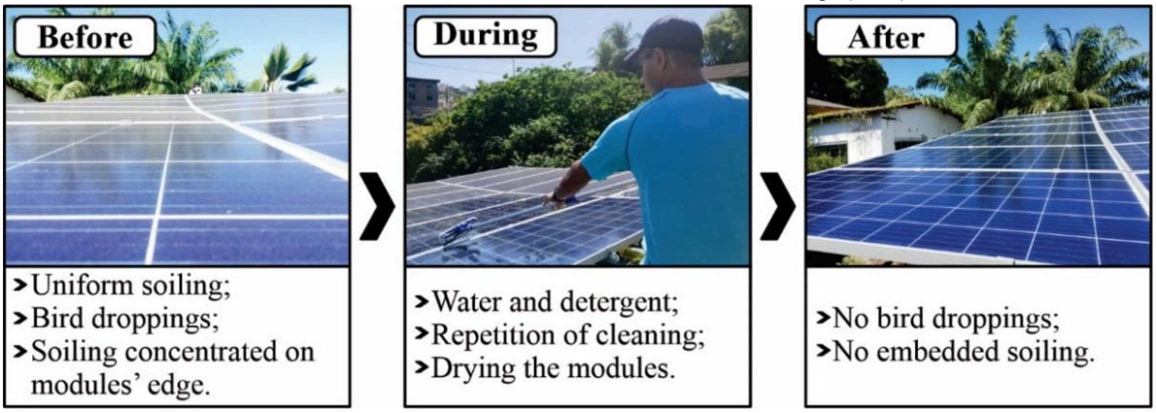

Fig. 2: LEA2 modules before, during and after 1st manual cleaning (July 5th, 2023).

After the first cleaning, only ST2 modules are subjected to new manual cleanings. The variation of the cleaning intervals aims to observe LEA2 electrical behavior in different rainfall regimes and periods of soiling exposure. LEA2 manual cleaning schedule is shown in Tab. 2.

Tab. 2: Schedule of LEA2 cleanings.

Year	Date
2023	July 5, 12, 19, 26; August 2, 26, 30; September 13, 27; October 18; November 8, 29; December 20
2024	January 10, 17, 31; February 7; March 6; April 3; May 8; June 12; July 17; August 7, 14, 28; September 18; October 16; November 20; December 11
2025	January 15

2.3. Analytical methods

In the Fixed Fill Factor Model (FFFM), the Fill Factor (FF) does not vary during the PV modules operation (Fuentes *et al*, 2007); thus, P_{Max} is determined by (eq. 1); V_{oc} and I_{sc} are calculated by (eq. 2) and (eq. 3), respectively (Anderson, 1996), where β is the temperature coefficient of V_{oc}, and δ is the correction coefficient of V_{oc} for irradiance; δ is determined by (eq. 4) (Batzelis, 2017).

$$P_{Max}=FF\cdot I_{sc}\cdot V_{oc} \quad \text{(eq. 1)}$$

$$V_{oc}=V_{oc_{STC}}\cdot[1+\beta(T_c - T_{STC})]\cdot\left[1+\delta\cdot \ln\left(\frac{G_{POA}}{G_{STC}}\right)\right] \quad \text{(eq. 2)}$$

$$I_{sc}=I_{sc_{STC}}\cdot[1+\alpha(T_c-T_{STC})]\cdot\frac{G_{POA}}{G_{STC}} \quad \text{(eq. 3)}$$

$$\delta=\frac{1-\beta(T_{STC}+273,15)}{50,1-\alpha(T_{STC}+273,15)} \quad \text{(eq. 4)}$$

In the Variable Fill Factor Model (VFFM) (Araujo; Sánchez, 1982), FF varies according to the PV modules operating conditions and can be determined by (eq. 5) - (eq. 8); V_{oc} and I_{sc} are calculated by (eq. 2) and (eq. 3), respectively. To determine P_{Max}, (eq. 1) is used, with FF value obtained by (eq. 5).

$$FF=FF_o\cdot\left(1-\frac{R_s}{\frac{V_{oc}}{I_{sc}}}\right) \quad \text{(eq. 5)}$$

$$R_s=\frac{V_{ocSTC}}{I_{scSTC}}\cdot\left(1-\frac{FF_{STC}}{FF_{oSTC}}\right) \quad \text{(eq. 6)}$$

$$FF_o=\frac{v_{oc}-\ln(v_{oc}+0,72)}{v_{oc}+1} \quad \text{(eq. 7)}$$

$$v_{oc}=\frac{V_{oc}}{k\cdot T_c}\cdot q \quad \text{(eq. 8)}$$

R_s is the series resistance, FF_o is the intrinsic fill factor, v_{oc} is the normalized open-circuit voltage, k is the Boltzmann constant ($1.38\cdot10^{-23}$ J K^{-1}), q is the charge of an electron ($1.602\cdot10^{-19}$ C) and T_c is the cell temperature in Kelvin (K); $FF_{o_{STC}}$ is the intrinsic fill factor in STC.

In the Approximate Maximum Power Point Model (AMPPM) (Araujo; Sánchez, 1982), the maximum voltage, current and power are estimated as a function of I_{sc} and V_{oc}, according to the following steps: (1) V_{oc} and I_{sc} are determined by (eq. 2) and (eq. 3); (2) r_s, a and b are calculated by (eq. 9) - (eq. 11); (3) I_{Max} and V_{Max} are determined by (eq. 12) and (eq. 13), respectively; and (4) P_{Max} is calculated by (eq. 14).

$$r_s=1-\frac{FF_{STC}}{FF_o} \quad \text{(eq. 9)}$$

$$a=v_{oc}+1-2\cdot v_{oc}\cdot r_s \quad \text{(eq. 10)}$$

$$b=\frac{a}{1+a} \quad \text{(eq. 11)}$$

$$I_{Max}=I_{sc}\cdot\left(1-a^{-b}\right) \quad \text{(eq. 12)}$$

$$V_{Max}=V_{oc}\cdot\left[1-\frac{b}{v_{oc}}\cdot\ln(a)-r_s\cdot(1-a^{-b})\right] \quad \text{(eq. 13)}$$

$$P_{Max}=V_{Max}\cdot I_{Max} \quad \text{(eq. 14)}$$

2.4. Soiling metrics extraction

To quantify soiling losses, the SRatio estimated is calculated from the relationship between the measured power ($P_{Max_{measured}}$) and the estimated power ($P_{Max_{estimated}}$), according to:

$$SRatio_{estimated}=\frac{P_{Max_{measured}}}{P_{Max_{estimated}}} \quad \text{(eq. 15)}$$

SRatio presents high variation; therefore, the following filters are used: (i) only measurements from 10 am to 2 pm are considered; (ii) irradiance must be ≥ 700 W/m^2, with variation of less than ±10% in a period of 10 minutes; (iii) data inconsistencies and/or absence of irradiance or power data are excluded; (iv) moments with cloudy sky conditions are disregarded. Sky conditions are classified into three distinct $k't$ (Modified Clearness Index) intervals: cloudy ($0 < k't \leq 0.3$), partly cloudy ($0.3 < k't \leq 0.65$) and clear ($0.65 < k't \leq 1$) (Amillo; Huld; Müller, 2014).

SRatio estimated by each of the analytical methods are compared with the SRatio measured:

$$SRatio_{measured}=\frac{P_{Max_{dirty}}}{P_{Max_{clean}}}\cdot K_{mismatch} \quad \text{(eq. 16)}$$

$K_{mismatch}$ represents the disparity of P_{Max} of the clean and dirty strings ($P_{Max_{clean}}$e $P_{Max_{dirty}}$), when both are under the same operating conditions. It is assumed that $K_{mismatch}$ remains constant during the experimental period, with a value of 1.04, obtained after manual cleaning of all modules.

2.5. Evaluation Metrics

To identify the analytical models with the highest accuracy and, consequently, the greatest applicability in estimating PV electrical parameters at the study site, the following evaluation metrics are employed: Mean Bias Error (MBE), Root Mean Squared Error (RMSE), Mean Absolute Percentage Error (MAPE), and Mean Percentage Error (MPE), as expressed in eq. (17) - (20), respectively. Where $y_i$is the measured value, $\hat{y}_i$is the estimated value, $\bar{y}$is the mean of the measured values, and $N$is the total number of measurements.

$$MBE=\frac{1}{N}\cdot\sum_{i=1}^{N}\left(y_i-\hat{y}_i\right) \quad \text{(eq. 17)}$$

$$RMSE=\sqrt{\frac{1}{N}\cdot\sum_{i=1}^{N}\left(y_i-\hat{y}_i\right)^2} \quad \text{(eq. 18)}$$

$$MAPE=\frac{1}{N}\cdot\sum_{i=1}^{N}\left|\frac{y_i-\hat{y}_i}{y_i}\right| \quad \text{(eq. 19)}$$

$$MPE=\frac{100\%}{N}\cdot\sum_{i=1}^{N}\frac{y_i-\hat{y}_i}{y_i} \quad \text{(eq. 20)}$$

3. Results and discussion

3.1. Applicability of analytical models at the study site

Since only ST2 is subjected to regular manual cleaning, the applicability study of the analytical models for determining electrical parameters is conducted exclusively with the measured and estimated values of this string. The analysis covers measurements taken between July 5th, 2023, and November 30th, 2024 (23,190 points for each variable are considered valid for analysis). Tab. 3 shows the values of the error metrics used to evaluate the analytical models to estimate the P_{Max} of ST2.

Tab. 3: Evaluation metrics for ST2 electrical parameter models.

Model	MBE	RMSE	MAPE	MPE (%)
FFFM	66.12	121.15	0.12	8.46
VFFM	-9.18	97.35	0.09	1.38
AMPPM	66.36	121.24	0.12	8.48

VFFM model presents the smallest errors in estimating ST2 power. According to the MAPE evaluation criteria established by Lewis (1982), FFFM and AMPPM models are classified as having good accuracy, with MAPE values between 0.10 and 0.20. VFFM stands out for its high accuracy, presenting a MAPE below 0.10.

To evaluate the compatibility of the analytical models under different sky conditions, three representative days are selected: (I) cloudy (02/06/2024 - $k't$ = 0.30); (II) partly cloudy (19/08/2023 - $k't$ = 0.33) and (III) clear (14/09/2023 - $k't$ = 0.63). Tab. 4 presents the error evaluation metrics of the analytical models for these conditions.

Tab. 4: Evaluation metrics of analytical models for representative cloudy, partly cloudy, and clear sky days.

Sky conditions	Model	*MBE*	*RMSE*	*MAPE*	*MPE (%)*
Cloudy (February 6th 2024)	FFFM	137.12	157.90	0.20	17.79
	VFFM	38.09	76.27	0.09	4.78
	AMPPM	137.30	158.04	0.20	17.81
Partly Cloudy (August 19th 2023)	FFFM	99.87	104.01	0.14	13.53
	VFFM	-14.72	51.54	0.05	1.07
	AMPPM	100.05	104.14	0.14	13.55
Clear (September 14th 2023)	FFFM	15.71	52.69	0.06	0.51
	VFFM	-59.13	80.02	0.10	9.57
	AMPPM	16.02	52.78	0.06	0.49

For cloudy skies, the best performance is observed for the VFFM model, which presents the lowest values across all metrics evaluated, particularly in MAPE (0.09) and MPE (4.78%). FFFM and AMPPM models exhibit similar behavior, but with significantly larger errors compared to the VFFM. For partly cloudy skies, the results are like those observed for cloudy skies. VFFM model again stands out, with a negative MBE value (-14.72), indicating a slight underestimation, and the lowest MAPE (0.05) and MPE (1.07%).

For clear skies, FFFM and AMPPM models exhibit similar behavior, with the lowest MAPE values (0.06). FFFM model slightly outperforms the MBE and RMSE metrics, while AMPPM demonstrates a slight advantage in the MPE metric. On the other hand, VFFM model presents the highest MBE (-59.13) and RMSE (80.02) values, indicating significant underestimation.

Overall, VFFM is the most accurate model under cloudy and partly cloudy conditions, but its performance declines under clear conditions. FFFM and AMPPM models excel under clear conditions, presenting the lowest errors in this situation. The models exhibit greater consistency in performance under clear conditions, while cloudy conditions result in greater dispersion in error metrics.

3.2. Estimation of soiling metrics through analytical models

SRatio values estimated through the analytical models and the respective SRatio values measured from the dirty and clean modules power are evaluated over a period of 18 months (from June 2023 to January 2025) and are presented in Fig. 3. SRatio values are calculated considering a weekly interval in relation to the performance of ST2 manual cleaning.

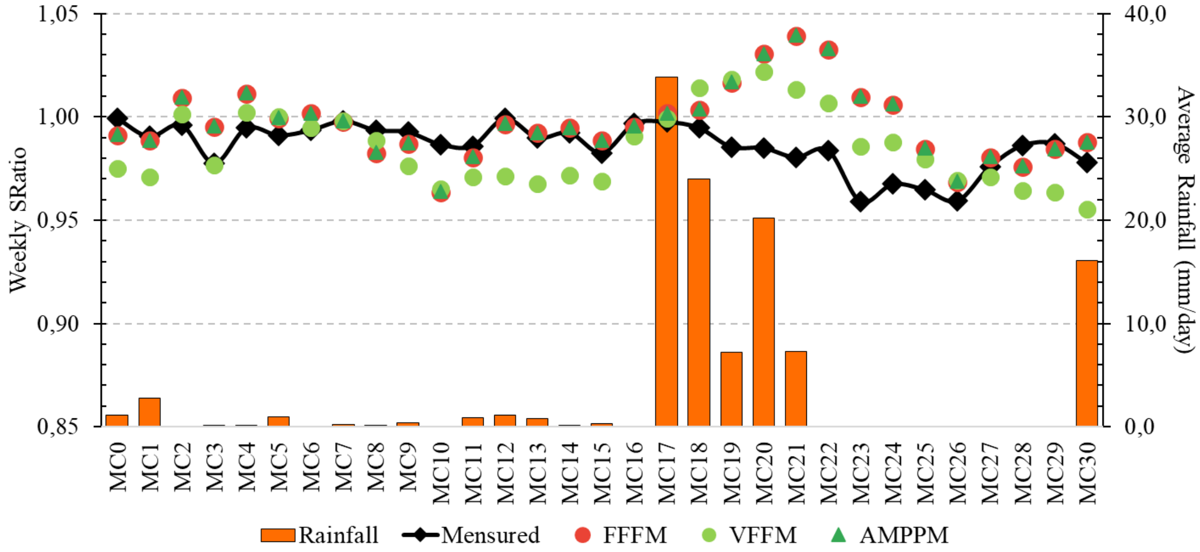

Fig. 3: Weekly values of measured and estimated SRatio.

SRatio values estimated by the FFFM, VFM, and AMPPM models approximate the measured values, with nearly identical results between the FFFM and AMPPM models. Over the entire analyzed period, the average difference between the estimated and measured values ranges from 0.07% for the VFFM model to -1.12% for the AMPPM model. Furthermore, all the methods analyzed are influenced by seasonality, especially in the LM17-LM24 period, when SRatio values are overestimated. During this period, the average difference compared to the measured values ranges from -4.81% for the FFFM model to -6.55% for the AMPPM model. Fig. 4 presents the metrics to assess the accuracy of the different analytical models in determining SRatio, calculated considering the full data set, covering the 18 months of the study's execution, which provides a comprehensive view of each model's performance.

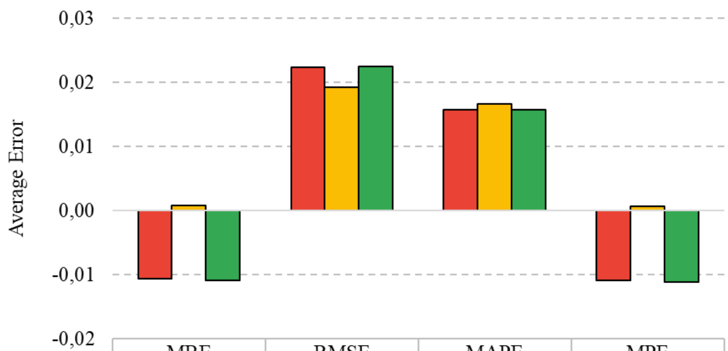

	MBE	RMSE	MAPE	MPE
FFFM	-0,01	0,02	0,02	-1,10%
VFFM	0,00	0,02	0,02	0,07%
AMPPM	-0,01	0,02	0,02	-1,12%

Fig. 4: Average error metrics of estimated SRatio relative to measured.

FFFM and AMPPM models show identical results for MBE, RMSE, and MAPE metrics: -0.01, 0.02, and 0.02, respectively. However, when analyzing the MPE metric, FFFM model performs slightly better than AMPPM, with an MPE of -1.10% compared to -1.12% for AMPPM. Overall, both models demonstrate similar performance, with low RMSE, MAPE, and MPE values, as well as a slight negative bias in the MBE (-0.01), making them suitable for applications that require less tolerance to absolute errors. In the overall analysis, VFFM model stands out as the most accurate and reliable, presenting the lowest MBE (0.00), indicating high precision with no tendency toward over- or underestimation. Furthermore, the RMSE (0.02) is slightly lower than that of the FFFM and AMPPM models, suggesting a smaller magnitude of errors. This balance between all metrics indicates VFFM as the best-performing model in the analyzed set.

FFFM and AMPPM methods exhibit medians of -0.60% and -0.63%, respectively, with less variation compared to ANM and SAPM. Although they still tend to underestimate results, these methods demonstrate greater precision and less dispersion. In turn, VFFM presents a median of 0.09%, demonstrating a low tendency for systematic errors, i.e., for underestimations or overestimations. Furthermore, data dispersion suggests a good balance between precision and accuracy, highlighting it as the most reliable model among those analyzed. Considering that the study site is in a region with irregular rainfall and that soiling losses tend to intensify during periods with fewer natural cleaning events, it is essential to evaluate the models performance considering the different rainfall periods, as illustrated in Fig. 5. This analysis allows to understand how the specific climatic conditions of each period influence the models behavior.

	MBE	RMSE	MAPE	MPE
FFFM	0,00	0,00	0,00	-0,20%
VFFM	0,02	0,02	0,02	1,97%
AMPPM	0,00	0,00	0,00	-0,22%

(a)

	MBE	RMSE	MAPE	MPE
FFFM	-0,02	0,03	0,02	-2,27%
VFFM	-0,02	0,03	0,02	-2,31%
AMPPM	-0,02	0,03	0,02	-2,30%

(b)

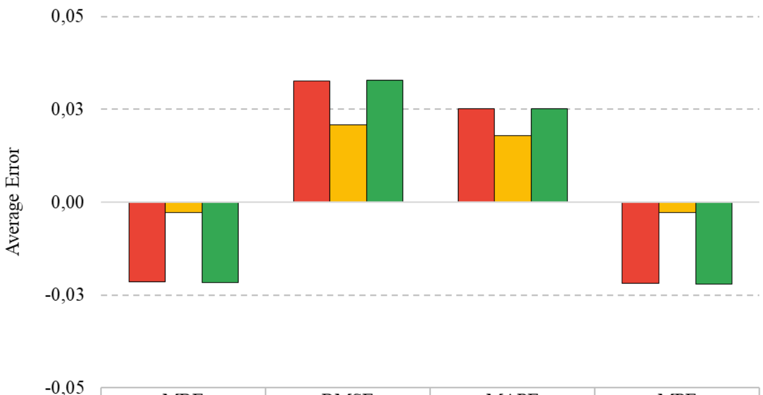

	MBE	RMSE	MAPE	MPE
FFFM	-0,02	0,03	0,03	-2,18%
VFFM	0,00	0,02	0,02	-0,28%
AMPPM	-0,02	0,03	0,03	-2,20%

(c)

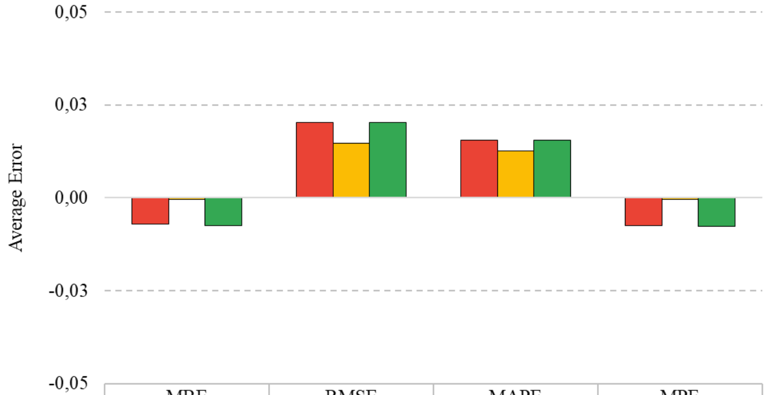

	MBE	RMSE	MAPE	MPE
FFFM	-0,01	0,02	0,02	-0,75%
VFFM	0,00	0,01	0,01	-0,05%
AMPPM	-0,01	0,02	0,02	-0,77%

(d)

Fig. 5: Error assessment metrics by rainfall period: (a) pre-rainy; (b) rainy; (c) post-rainy; (d) dry.

During the pre-rainy season, the models exhibit relatively low error values, particularly for FFFM and AMPPM, which record the lowest values across all metrics evaluated, indicating greater accuracy compared to the other models. During the rainy season, FFFM, VFFM, and AMPPM models exhibit similar behavior across all metrics and maintain better relative performance, with MAPE and MPE below -3%, demonstrating greater consistency.

During the post-rainy season, the error patterns are like those of the previous season, particularly for VFFM, which records a consistent reduction of MBE and MPE compared to the rainy season. FFFM and AMPPM models maintain stable behavior, with a slight reduction of MPE and a small increase of MAPE, demonstrating resilient performance. During the dry season, FFFM, VFFM, and AMPPM models show a reduction of error metrics, with VFFM outperforming the others in all metrics evaluated. This analysis highlights the influence of seasonal conditions on model performance and underscores the importance of considering these variations when assessing soiling effects on PV plant performance under different rainfall regimes.

4. Conclusion

Summarizing, FFFM and AMPPM models are more accurate in estimating soiling losses during the pre-rainy season. In periods with lower precipitation levels (post-rainy and dry seasons), VFFM model performs better. During the rainy season, FFFM, VFFM, and AMPPM models exhibit similar performance, with FFFM slightly ahead. Therefore, the analysis demonstrates that FFFM, VFFM, and AMPPM analytical models have the potential to be used in an integrated manner for real-time soiling losses estimation in PV plants, based on a limited set of input data: power, irradiance, and T_m. However, seasonality exerts a significant influence on all models. These results reinforce the importance of considering local environmental conditions when calibrating models to improve their applicability to soiling studies.

5. Acknowledgments

The work of José Janiere S. de Souza was supported by the Federal Institute of Ceará (IFCE)–Campus Cedro, through the granting of a leave of absence to pursue his Ph.D. Paulo C. M. Carvalho thanks the National Council for Scientific and Technological Development (CNPq) for a Research Scholarship.

6. References

Ahmadullah, A. B., Bakhtyal, I. A., Irshad, A. S., Doost, Z. H., Wali, N., & Karimi, B. A, 2026. Comparative assessment of optimal cleaning schedules for various PV cleaning techniques. Renewable Energy, 256, https://doi.org/10.1016/j.renene.2025.124182.

Amillo, A.G., Huld, T., Müller, R., 2014. A new database of global and direct solar radiation using the eastern meteosat satellite, models and validation. Remote Sens (Basel) 6. https://doi.org/10.3390/rs6098165.

Anderson, A.J., 1996. Photovoltaic translation equations: A new approach. NREL, Golden.

Araujo, G.L., Sánchez, E., 1982. Analytical expressions for the determination of the maximum power point and the fill factor of a solar cell. Solar Cells 5, 377–386. https://doi.org/10.1016/0379-6787(82)90008-4.

Assis, D. P. D., Santos, L. D. O., Pereira, R. I. S., De Souza, J. J. S., & Carvalho, P. C. M. D. (2025). Scalable data acquisition system for real-time monitoring of photovoltaic plants. *IEEE Access*, 1. doi:10.1109/access.2025.3609654.

Batzelis, E.I., 2017. Simple PV Performance Equations Theoretically Well Founded on the Single-Diode Model. IEEE J Photovolt 7, 1400–1409. https://doi.org/10.1109/JPHOTOV.2017.2711431

Bessa, J. G., Micheli, L., Almonacid, F., and Fernández, E. F. (2021). Monitoring photovoltaic soiling: Assessment, challenges, and perspectives of current and potential strategies. *IScience*, *24*(3), 102165. doi:10.1016/j.isci.2021.102165.

Brunel, F., López, R., García, F., Peters, E., & Funes, G. (2025). Estimation of the power loss of a soiled photovoltaic panel using image analysis techniques. *Energies*, *18*(18), 4889. doi:10.3390/en18184889.

Conceição, R., González-Aguilar, J., Merrouni, A. A. and Romero, M. (2022). Soiling effect in solar energy conversion systems: A review. *Renewable and Sustainable Energy Reviews*, *162*, 112434. doi:10.1016/j.rser.2022.112434.

Cruz-Rojas, T., Franco, J. A., Hernandez-Escobedo, Q., Ruiz-Robles, D., & Juarez-Lopez, J. M. (2023). A novel comparison of image semantic segmentation techniques for detecting dust in photovoltaic panels using machine learning and deep learning. *Renewable Energy*, 119126. doi:10.1016/j.renene.2023.119126.

Fernández-Solas, Á., Montes-Romero, J., Micheli, L., Almonacid, F., Fernández, E.F., 2022. Estimation of soiling losses in photovoltaic modules of different technologies through analytical methods. Energy 244, 123173. https://doi.org/10.1016/j.energy.2022.123173

Ferrada, P., Olivares, D., del Campo, V., Marzo, A., Araya, F., Cabrera, E., ... Fuentealba, E., 2019. Physicochemical characterization of soiling from photovoltaic facilities in arid locations in the Atacama Desert. *Solar Energy*, *187*, 47–56. doi:10.1016/j.solener.2019.05.034

Fuentes, M., Nofuentes, G., Aguilera, J., Talavera, D.L., Castro, M., 2007. Application and validation of algebraic methods to predict the behaviour of crystalline silicon PV modules in Mediterranean climates. Solar Energy 81, 1396–1408. https://doi.org/10.1016/j.solener.2006.12.008.

Jones, R. K., Baras, A., Saeeri, A. A., Al Qahtani, A., Al Amoudi, A. O., Al Shaya, Y., ... Al-Hsaien, S. A., 2016. Optimized cleaning cost and schedule based on observed soiling conditions for photovoltaic plants in central saudi arabia. *IEEE Journal of Photovoltaics*, *6*(3), 730–738. doi:10.1109/jphotov.2016.2535308

Lewis, C. D. Industrial and business forecasting methods: a practical guide to exponential smoothing and curve fitting. 1982. London: Butterworth Scientific, 143 p. ISBN 0408005599.

Souza, J. J. S. de and Carvalho, P. C. M., 2025. Experimental investigation of the soiling impact on the generation of a photovoltaic plant in an urban area of the Brazilian semiarid. *Sustainable Energy Technologies and Assessments*, *73*, 104153. doi:10.1016/j.seta.2024.104153.

Souza, J. J. S., Carvalho, P. C. M., and Barroso, G. C., 2022. Analysis of the characteristics and effects of soiling natural accumulation on photovoltaic systems: A systematic review of the literature. *Journal of Solar Energy Engineering*, 1–99. doi:10.1115/1.4056453.

Souza, J. J. S., Carvalho, P. C. M., and Pereira, R. I. S., 2023. Efeitos da sujidade no desempenho elétrico de uma planta fotovoltaica: Um estudo de caso no LEA-UFC. *Conexões - Ciência e Tecnologia*, *17*, Artigo e022011. doi:10.21439/conexoes.v17i0.2724.

Souza, J. J. S. ; Santos, L. O. ; Carvalho, P. C. M., 2025. Influence of Manual Cleaning on the Thermal Behavior of Photovoltaic Modules. *IEEE Access*, v. 13, p. 85231-85238. 10.1109/ACCESS.2025.3570217.